

Milan Kuchta; O. Čadek; G. Tobie

Thermal convection in a rotating spherical body with free surface:
Implications for Saturn's moon iapetus

Acta Universitatis Carolinae. Mathematica et Physica, Vol. 53 (2012), No. 2, 87--95

Persistent URL: <http://dml.cz/dmlcz/143703>

Terms of use:

© Univerzita Karlova v Praze, 2012

Institute of Mathematics of the Academy of Sciences of the Czech Republic provides access to digitized documents strictly for personal use. Each copy of any part of this document must contain these *Terms of use*.



This paper has been digitized, optimized for electronic delivery and stamped with digital signature within the project *DML-CZ: The Czech Digital Mathematics Library* <http://project.dml.cz>

THERMAL CONVECTION IN A ROTATING SPHERICAL BODY WITH FREE SURFACE: IMPLICATIONS FOR SATURN'S MOON IAPETUS

M. KUCHTA, O. ČADEK, G. TOBIE

Praha, Nantes

Received June 11, 2012

Revised October 10, 2012

We present a new numerical tool to simulate thermal cooling and spin evolution of a rotating body with freely deformable surface and complex rheology. While the long-term mechanical properties of the body are mimicked by visco-plastic rheology including different creep mechanisms, its despinning is controlled by Andrade visco-elastic model. Variable-density approximation (sticky air) and implicit description of the surface are combined in order to track the surface evolution. We use this tool to investigate the shape of Saturn's moon Iapetus, whose topography shows enigmatic remnant features from the moon's early history when the spin rate and temperature were significantly higher than at present. Our model is characterized by three parameters: the initial temperature (ranging from 230 to 270 K), the initial rotational period (8–15 hours), and the grain size of ice (0.01–100 mm) defining the relative role of diffusion creep in total deformation. For these three parameters, we systematically explore the model space and show for which combinations of parameters the body can be effectively despun while maintaining its strongly flattened shape. Our results indicate that the despinning of Iapetus could not occur without interaction with an external body.

1. Introduction

The topography of Iapetus, the most distant of Saturn's major icy moons, shows two enigmatic features: an exceptionally large equatorial bulge and a narrow equatorial ridge reaching heights of ~ 13 km above the surrounding terrain. According to *Thomas et al.* [2007], the strongly flattened shape with equatorial radius 747.4 ± 3.1 km and polar radius 712.4 ± 2.0 km corresponds to a rotational period of ~ 16 h

Department of Geophysics, Faculty of Mathematics and Physics, Charles University, Prague
Laboratoire de Planétologie et Géodynamique de Nantes Université de Nantes, Nantes, France

The work was supported by project SVV-2012-265308.

Key words and phrases. thermal convection, Iapetus

E-mail address: miroslav.kuchta@gmail.com

for a homogeneous body or ~ 15 h for a differentiated body. However, the current synchronous rotational period is 79.33 days. The equatorial ridge is located at the top of the bulge and runs nearly parallel to the equator on the leading dark side of Iapetus. Recently, *Giese et al.* [2008] have detected signs of the ridge also on the trailing bright hemisphere. Heavy cratering of the ridge, which indicates an ancient origin, and further its location on top of the bulge are suggestive of a causal link between the two features, see e.g. *Czechowski and Leliwa-Kopystynski* [2008], *Levison et al.* [2011], *Sandwell and Schubert* [2010], *Castillo-Rogez et al.* [2007].

In this paper we consider the hypothesis of *Castillo-Rogez et al.* [2007] who proposed that the present-day shape of Iapetus is a remnant from the times when the moon rotated with a high spin rate and whose preservation was made possible by creation of a lithosphere strong enough to resist deformations due to continuing despinning. For the formation of the lithosphere, as well as for the onset of the despinning, heat from the decay of short-lived radiogenic isotopes (SLRI) was crucial. The scenario does not describe the formation of the ridge, but in their simulations with a model that included 1-D purely conductive heat transfer and Maxwell rheology, the authors used the presence of the ridge as a constraint on the strength and width of admissible lithosphere. The scenario was also investigated by *Robuchon et al.* [2010] on the basis of 3-D convection simulations incorporating a highly dissipative Burgers rheology. Despite the differences in modeling strategies, both *Castillo-Rogez et al.* [2007] and *Robuchon et al.* [2010] were able to successfully despin Iapetus and obtain the correct flattening. The models are, however, strongly simplified: The model of *Castillo-Rogez et al.* [2007, 2011] neglects the effect of convective cooling while the model of *Robuchon et al.* [2010] oversimplifies the rheological description of viscous flow and tidal dissipation. Here we devise a new model where the aforementioned drawbacks are eliminated.

2. Model

2.1 Governing equations

We consider a flow of highly viscous, incompressible fluid driven by thermally dependent buoyancy forces. Governing equations of our model therefore constitute a Stokes-Fourier system

$$(1) \quad \left. \begin{aligned} \nabla \cdot \vec{v} &= 0 \\ -\nabla \pi + \nabla \cdot (\eta (\nabla \vec{v} + (\nabla \vec{v})^T)) + \rho (\vec{g} + \vec{b}) &= 0 \\ \rho_m c_p \left(\frac{\partial T}{\partial t} + \vec{v} \cdot \nabla T \right) &= \nabla \cdot (k \nabla T) + q \\ \rho &= \rho_m (1 - \alpha (T - T_m)), \quad \alpha = \text{const} > 0 \end{aligned} \right\} \Omega_t \times (0, T),$$

where \vec{v} is the velocity of the flow, π is the Lagrange multiplier that ensures incompressibility and η, ρ, k, c_p and α are respectively the fluid's viscosity, density, thermal conductivity, specific heat and expansion coefficient, T is the thermodynamic temperature, T_m is the reference temperature at which density takes the value ρ_m , \vec{g} is the gravitational acceleration, \vec{b} is the centrifugal acceleration and q is the volumetric radiogenic heat production. The equations are prescribed in domain Ω_t corresponding to the real shape of Iapetus.

Following *Castillo-Rogez et al.* [2007] our model includes temperature-dependent thermal parameters k and c_p that are given by

$$(2) \quad \begin{aligned} k &= f_s k^{\text{sil}} + (1 - f_s) k^{\text{ice}}, \quad k^{\text{ice}} \left[\text{Wm}^{-1} \text{K}^{-1} \right] = 0.4685 + 488.12/T, \\ c_p &= \chi_s c_p^{\text{sil}} + (1 - \chi_s) c_p^{\text{ice}}, \quad c_p^{\text{ice}} \left[\text{J kg}^{-1} \text{K}^{-1} \right] = 185 + 7.037T, \end{aligned}$$

where $k^{\text{sil}} = 4.2 \text{ Wm}^{-1} \text{K}^{-1}$, $c_p^{\text{sil}} = 920 \text{ J kg}^{-1} \text{K}^{-1}$ are the thermal conductivity and specific heat of the silicates. In equations (2), $f_s = 0.063$ and $\chi_s = 0.204$ are the volumetric and mass fraction of the silicates, respectively [*Robuchon et al.*, 2010].

2.2 Rheology

Goldsby and Kohlstedt [2001] showed that for a realistic description of the deformation of ice a single deformation mechanism is not sufficient. Instead, combination of several different mechanisms yields results that are in excellent agreement with experiments. They considered four such mechanisms: dislocation creep, diffusion creep, basal slip and grain boundary sliding. Viscosity corresponding to each of the mechanisms follows an Arrhenius-like flow law

$$(3) \quad \eta_i = \frac{1}{2} \dot{\epsilon}_{II}^{-1+1/n_i} d^{p_i/n_i} \left[A_i + \exp\left(-\frac{E_i}{RT}\right) \right]^{-1/n_i}.$$

The dependence of mechanism's viscosity on the second invariant of the strain-rate tensor $\dot{\epsilon}_{II}$, grain size d and temperature is thus controlled by its the grain-size exponent p_i , stress exponent n_i , pre-exponential factor A_i and activation energy E_i . In Equation 3 R is the universal gas constant. We adopt values of parameters characterizing individual mechanisms from *Goldsby and Kohlstedt* [2001] but unlike the authors, we consider all the mechanisms in series. Hence, the final viscosity is given as

$$(4) \quad \frac{1}{\eta} = \sum_i \frac{1}{\eta_i}.$$

2.3 Despinning

Despite the large distance from Saturn (semi-major axis $D = 3.51 \times 10^6$ km), Iapetus experienced non-zero tidal forces induced by the gravitational field of Saturn.

The evolution of spin rate ω is then given by *Peale* [1999]

$$(5) \quad \frac{d\omega}{dt} = -\frac{45}{16\pi} \frac{k_2(t) GM_p^2 a(t)}{\rho D^6 Q(t) c(t)},$$

where M_p is the Saturn’s mass, k_2 is the tidal Love number, Q is the quality factor characterizing the dissipation of energy in visco-elastic deformation, G is the gravitational constant and a and c are the moon’s equatorial and polar radius, respectively. In our model, anelastic properties of Iapetus are described by Andr ade visco-elastic model *Efroimsky* [2012]. The evolution of spin rate is coupled to the Stokes problem via centrifugal force which influences the character of flow and the shape of the body. Especially at high spin rates, mass redistribution due to changes in shape is significant. Consequently, self-gravity must be included in the gravitational force.

2.4 Model domain, surface evolution and boundary conditions

In order to reduce the computational costs we introduce two simplifications. First, we do not consider a 3-D spherical domain, but instead, we perform our calculations in a 2-D axisymmetric spherical geometry which represents an intersection between the slice of Iapetus passing through rotational axis and the half-plane determined by this axis and an arbitrary point in space. This simplification is well justified by the rotational symmetry of both the investigated phenomena.

Since the outer boundary of this domain represents an evolving surface, the force acting on it should be $\mathcal{S} \cdot \vec{n} = \vec{0}$, with \mathcal{S} and \vec{n} being the Cauchy stress tensor and the outer unit normal, respectively. The condition allows the surface to deform freely but substantial computational expanses arise upon its implementation due to accurate evaluation of surface normals at each time step. Further, if Eulerian description is used, the evolving surface affects size of the matrix of the problem, as the number of Eulerian nodes that are part of the physical/computational domain changes with time. To avoid the highly demanding assembly of the matrix at each time step, we use the variable-density approximation where the computational domain is fixed (together with the dimension of the problem matrix) and its volume is sufficiently large to contain the physical domain throughout the whole time evolution. The additional volume above the physical surface is then filled with material whose properties allow the physical surface to deform freely. In this approximation, the physical surface is identical to the interface between the two materials – ice within the physical domain and a low-viscosity and low-density “sticky air” above it. In our model, we describe the interface as an implicit function $H(r, \theta, t) = 0$ whose evolution is an initial-boundary-value problem with the governing equation

$$(6) \quad \frac{\partial H}{\partial t} + \vec{v} \cdot \nabla H = 0.$$

Since in variable-density approximation the fixed boundary of the computational domain does not coincide with the evolving boundary of the physical domain, simplified boundary conditions can be used on the outer boundary. In our simulations, we prescribed here a free-slip condition and constant temperature of 90 K. On the inner boundary free-slip and zero heat flux were used. Finally, on the axial boundaries conditions requiring symmetry of velocity, temperature and surface were prescribed.

2.5 Model space exploration

The initial state of Iapetus, characterized by an initial temperature profile $T_0(r, \theta)$, rotational period τ_0 and grain size d , is largely unknown. To estimate the initial conditions which are compatible with the present-day flattening and rotational period, we test different combinations of the above initial parameters by simulating the thermal evolution of the moon. For each set of parameters we obtain spin rate and flattening as functions of time and we compare them with the present values. We consider the initial rotational period between 8 and 15 hours, which corresponds to initial flattening $a - c$ between 170 km and 40 km. For these values of periods, *Robuchon et al.* [2010] were able to successfully despin Iapetus and obtain the observed flattening. It should be noted, that while investigation of bigger initial rotational periods is likely unnecessary due to correspondence between the current shape and 16-hour rotational period, values as small as Roches's limit of 4 h should be included in numerical simulations. However, at the moment of writing such simulations are outside the authors' computational capabilities.

We vary the grain sizes between 0.01 mm and 100 mm, in agreement with the values given by *Czechowski and Leliwa-Kopystynski* [2008] who studied convection in mid-sized icy satellites (the effect of grain size is illustrated in the top panel of Figure 1).

Finally, we consider high constant initial temperature $T_0 \in [230 \text{ K}, 270 \text{ K}]$ in order to aid the dissipation. The temperature is assumed to result from initial accretion processes and the radiogenic decay of SLRI. We assume that at the start of numerical simulations all SLRI are burned out and it is only the LLRI that keep heating the interior up. Moreover, following *Robuchon et al.* [2010], we assume no internal differentiation of Iapetus and hence the heating to be homogeneous. Initial amount of LLRI then depends on the time difference Δt between accretion and the simulation start. Nevertheless, since half-lives of the dominant LLRI are close to 1 Byr the effect of Δt on radiogenic heating is negligible. In the presented results we set $\Delta t = 10 \text{ Myr}$.

3. Results

We investigated the discretized model space

$$(d, \tau_0, T_0) \in \{0.01, 0.1, 1.0, 10.0, 100.0\} \text{ mm} \times \{8, 12, 15\} \text{ h} \times \{230, 250, 270\} \text{ K}.$$

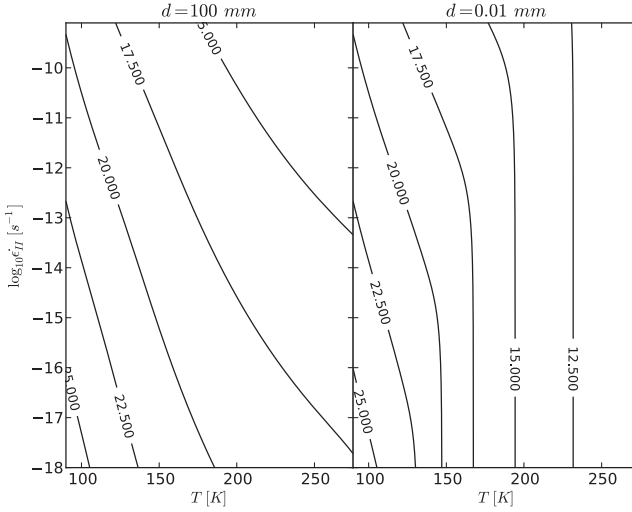
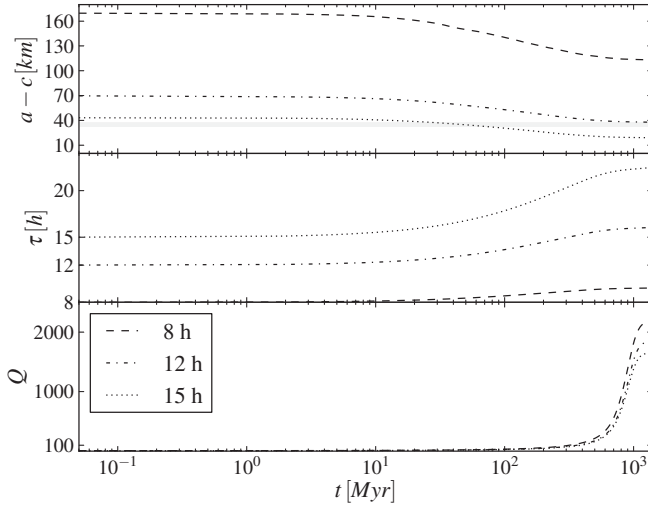


FIGURE 1. (Top) Contour maps of decadic logarithm of viscosity in Pa s as a function of strain rate and temperature for two boundary values of grain sizes considered in the study. For the largest grain size low viscosity regions are confined to large values of temperatures and strain rates. For the smallest grain size, low viscosities are obtained at $T > 230$ K independent of the strain-rate suggesting that viscosity is controlled by the diffusion creep. (Bottom) Evolution of flattening, rotational period and dissipation factor for model with $d = 0.1$ mm, $T_0 = 230$ K and three different values of τ_0 . In the first plot shaded gray region indicates confidence interval of the measurements of the current flattening of Iapetus $a - c = 35.0 \pm 3.7$ km [Thomas et al., 2007].

TABLE 1. Rotational periods (gray columns) and flattening (white columns) obtained after 1 Byr for models with grain size 100 mm and 0.01 mm.

d		100 mm						0.01 mm					
τ_0		8 h		12 h		15 h		8 h		12 h		15 h	
T_0		8 h	140 km	13.4 h	55 km	17.2 h	33 km	9.8 h	106 km	16.6 h	35 km	28.0 h	12.3 km
230 K		8.7 h	140 km	13.4 h	55 km	17.2 h	33 km	9.8 h	106 km	16.6 h	35 km	28.0 h	12.3 km
250 K		8.9 h	131 km	14.1 h	50 km	18.5 h	28 km	9.9 h	105 km	17.6 h	31 km	28.1 h	12.1 km
270 K		9.0 h	128 km	14.6 h	46 km	19.4 h	25 km	9.9 h	104 km	17.9 h	30 km	28.6 h	11.7 km

Between individual elements of the model space there are significant differences in initial flattening and viscosity that are induced by initial rotational period, initial temperature and grain size. Despite this fact, the models share common characteristics. There is a trade-off between the achieved rotational period and the obtained flattening. In Figure 1 (bottom), the flattening becomes constant for all initial rotational periods after ~ 800 Myr suggesting that the shape is frozen. Flattening of the model with $\tau_0 = 12$ hours is in very good agreement with the measurements. However, neither of the models despin into synchronous rotation – the corresponding rotational periods never exceeded 25 hours. Moreover, at $t > 800$ Myr all the models dissipate only a little energy ($Q > 1000$) and thus are unlikely to despin even if time intervals longer than 1 Byr were investigated.

The trade-off is apparent also in Table 1 which represents a summary of our results. As the response of the models is monotonous in grain size, we present outputs obtained only for the end-member values of d . For grain size $d = 100$ mm, the rotational period varies between $\tau = 8.7$ hours and $\tau = 19.4$ hours and the final flattening $a - c$ ranges from 140 km to 25 km. In models with the smallest grain size, viscosity η drops to a value of 10^{12} Pa s (cf. Figure 1). As a result, the interior is more dissipative and larger rotational periods are achieved ($\tau = 28.6$ hours for the model with $\tau_0 = 15$ hours and $T_0 = 270$ K), but, at the same time, the strength of the lithosphere is decreased and the obtained flattening is small ($a - c \sim 12$ km for the models with $\tau_0 = 15$ hours). Still, the rotational periods obtained for the smallest grain size are much smaller than the present-day period of 79.33 days.

4. Conclusions

Successful despining of Iapetus requires a relatively low value of quality factor Q . Such a value can only be obtained for very low values of viscosity, corresponding to high temperatures and/or small grain sizes. In turn, viscosity is the parameter controlling the thermal evolution of the interior: if the viscosity is too low, the body cools quickly and its temperature decreases. This leads to an increase of Q and a less efficient despining. To predict a correct final rotational period, the cooling must be

rather slow to keep the body warm and dissipative for sufficiently long time, and, at the same time, the viscosity must be large enough for the flattening to be preserved.

In all the models we have investigated, the heat transfer is mainly convective. More importantly, due to high initial temperatures, the convection is very vigorous in the early stage which leads to a fast cooling of the interior. As a consequence, the despinning is quickly suppressed and the rotational period is locked at a value that is much smaller than that observed at present. The question is whether low initial temperatures could give more promising results. Figure 1 suggests that for temperatures smaller than 180 K, Iapetus would cool by pure conduction. This temperature corresponds to viscosity 10^{17} Pa s which is considered to be a limit value for the onset of convection. However, such a value of viscosity would provide sufficiently small values of Q only for rotational periods that are significantly larger than the period of 16 hours corresponding to the present day flattening.

In contrast to the previous studies by *Castillo-Rogez et al.* [2007] and *Robuchon et al.* [2010], which used simplified cooling models or strongly simplified rheology, our results suggest that the despinning of Iapetus could not occur only due to tidal dissipation. Gravitational interaction with an external body or collision with a mid-size ($R > 50$ km) body was thus necessary to slow down, at least partially, the spin rate of Iapetus. Once the rotational period increased above certain limit, the despinning due to tidal forces became efficient even for low internal temperature which eventually led to the synchronous rotation of Iapetus that we observe today.

References

- CASTILLO-ROGEZ, J. C., EFROIMSKY, M., AND LAINEY, V.: The tidal history of Iapetus: Spin dynamics in the light of a refined dissipation model, *J. Geophys. Res.*, 116, E09 008, 2011.
- CASTILLO-ROGEZ, J. C., MATSON, D. L., SOTIN, C., JOHNSON, T. V., LUNINE, J. I., AND THOMAS, P. C.: Iapetus' geophysics: Rotation rate, shape, and equatorial ridge, *Icarus*, 190, 179–202, 2007.
- CZECHOWSKI, L. AND LELIWA-KOPYSTYNSKI, J.: The Iapetus's ridge: Possible explanations of its origin, *Adv. Space Res.*, 42, 61–69, 2008.
- EFROIMSKY, M.: Tidal dissipation compared to seismic dissipation: in small bodies, aarths, and super-aarths, *Astron. J.*, 746, 150, 2012.
- GIESE, B., DENK, T., NEUKUM, G., ROATSCH, T., HELFENSTEIN, P., THOMAS, P. C., TURTLE, E. P., MCEWEN, A., AND PORCO, C. C.: The topography of Iapetus' leading side, *Icarus*, 193, 359–371, 2008.
- GOLDSBY, D. L. AND KOHLSTEDT, D. L.: Superplastic deformation of ice: Experimental observations, *J. Geophys. Res.*, 106, 11017–11030, 2001.
- LEVISON, H. F., WALSH, K. J., BARR, A. C., AND DONES, L.: Ridge formation and de-spinning of Iapetus via an impact-generated satellite, *Icarus*, 214, 773–778, 2011.
- PEALE, S. J.: Origin and evolution of the natural satellites, *Annu. Rev. Astron. Astrophys.*, 37, 533–602, 1999.
- ROBUCHON, G., CHOBLET, G., TOBIE, G., CADEK, O., SOTIN, C., AND GRASSET, O.: Coupling of thermal evolution and despinning of early Iapetus, *Icarus*, 207, 959–971, 2010.

- SANDWELL, D. AND SCHUBERT, G.: A contraction model for the attenuing and equatorial ridge of Iapetus, *Icarus*, 210, 817–822, 2010.
- THOMAS, P. C., BURNS, J. A., HELFENSTEIN, P., SQUYRES, S., VEVERKA, J., PORCO, C., TURTLE, E. P., McEWEN, A., DENK, T., GIESE, B., ROATSCH, T., JOHNSON, T. V., AND JACOBSON, R. A.: Shapes of the saturnian icy satellites and their significance, *Icarus*, 190, 573–584, 2007.